LAWRENCE
LIVERMORE
NATIONAL
LABORATORY

LLNL-JRNL-642412

Quantifying Membrane Protein Interactions in Solution using Fluorescence Correlation Spectroscopy

S. Ly, F. Bourguet, N. O. Fischer, E. Y. Lau, M. A. Coleman, T. A. Laurence

August 15, 2013

Biophysical Journal

Disclaimer

Quantifying Membrane Protein Interactions in Solution using Fluorescence Correlation Spectroscopy

Sonny Ly[1], Feliza Bourguet[1], Nicholas O. Fischer[1], Edmond Y. Lau[1], Matthew A. Coleman[1,2], Ted A. Laurence[1]

[1]Lawrence Livermore National Laboratory, Livermore, CA 94550
[2]University of California, Davis, Department of Radiation Oncology, Sacramento, CA 95817

Using fluorescence correlation spectroscopy (FCS), we measured a dissociation constant of 22 nM between EGFP-labeled *Y. pestis* protein LcrV and its cognate membrane-bound protein YopB inserted into a nanolipoprotein (NLP) scaffold. The combination of FCS and NLP technologies provides a powerful approach to accurately measure binding constants of interactions between membrane bound and soluble proteins. Straightforward sample preparation, acquisition, and analysis procedures make this combined technology attractive for wide applicability.

Interactions involving membrane proteins are integral to a multitude of cellular processes, including signal transduction, energy production and conversion, cell adhesion, and foreign molecule identification. More than half of all pharmaceutical drugs target membrane proteins, further illustrating their importance in human health[1]. Due to this, there is a continuing high demand for methods that can screen, validate, and quantify interactions involving membrane proteins. Unfortunately, the quantitative techniques available to characterize protein-protein interactions are most often directed towards soluble proteins, and are often difficult to apply to membrane proteins[2]. Recently, advances in synthetic NLP technology, often referred to as lipid nanodiscs or reconstituted HDLs, have enabled biophysical and biochemical studies of membrane proteins[3]. The native-like lipid environment of NLPs maintains protein functionality, opening a realm of possibilities in analyzing membrane protein dynamics in solution.

NLPs are discoidal cell membrane mimetics 8-20 nm in diameter, consisting of a lipid bilayer stabilized by two peripheral apolipoprotein A-I (apoA-I) scaffold proteins[4]. NLPs provide an excellent alternative to traditional lipid-based platforms (e.g. liposomes) for membrane protein solubilization and interrogation. NLP diameter can be engineered by varying lipid composition to accommodate different-sized membrane proteins. As such, NLPs represent an important platform for expression, isolation, and study of functional membrane proteins and the multi-protein complexes they form. Several groups have successfully reconstituted a variety of membrane proteins, including GPCRs[5, 6], cytochrome P450[7], and secYEG channel[8]. NLPs may also be a suitable alternative to liposomes as targeted drug transport vehicles[9]. To produce solubilized, discrete membrane proteins, we utilized a cell-free expression approach to embed membrane proteins directly into NLPs formed in situ. This approach improves expression yields of soluble membrane-bound protein and can be applied to membrane proteins where

traditional approaches are unsuccessful.[10, 11] FCS analysis coupled with NLP technology has been successfully used to monitor small ligand binding interactions[6, 11] with membrane proteins and to measure lipid-protein interactions[12]. Here, we show that FCS combined with the cell-free production of membrane proteins directly into NLPs can be used to measure interactions between soluble proteins and cognate membrane proteins.

FCS uses correlation analysis of fluorescence arising from randomly diffusing molecules to measure diffusion constants, and hence hydrodynamic radii, of species in solution. Diffusion times measured by FCS are inversely proportional to diffusion constants. A shift to slower diffusion time indicates an increase in the hydrodynamic radius due to binding. Due to this size sensitivity, FCS has been proposed repeatedly as a method to quantify molecular interactions in solution[13]. However, an important difficulty in FCS arises when characterizing interactions between two proteins of similar size. The diffusion time is inversely proportional to the cube root of the molecular weight $\tau_D \sim M^{-1/3}$. Doubling the mass results in only in a factor of 1.3 increase in diffusion time, but a factor of 1.6 is required to resolve two species[14]. As we demonstrate, this difficulty is overcome by using FCS to measure the interactions between labeled soluble proteins and membrane proteins supported within NLPs. The much larger size of the membrane protein:NLP complex (M.W. 250kDa in the YopB-NLP example, Figure 1A) relative to most soluble proteins provides the necessary differential in diffusion times to easily resolve bound and free species by FCS.

Binding kinetics are readily measured using FCS by titrating increasing amounts of unlabeled cognate protein, resulting in a series of autocorrelation curves similar to those modeled in theoretical example in Figure 1B. For 0% binding (black curve), only the labeled soluble protein is present, producing in a single component correlation curve with a diffusion time of 0.1 ms. On the autocorrelation curve with a single component, the diffusion time is the time at which the autocorrelation amplitude decreases by half. For 100% binding (cyan curve), the amount of NLP with inserted membrane protein is well above the dissociation constant so that all available soluble protein is bound. Again a single component correlation curve is found, but now with a longer 10 ms diffusion time. Intermediate cases have two components, corresponding to free and bound protein. The relative amplitudes of the components obtained by fitting to two component models in these cases can be used to obtain a binding curve (Online Methods).

We investigated by FCS the interaction of two *Y. pestis* proteins: soluble EGFP-labeled LcrV and membrane-bound YopB (Figure 1A). YopB is an effector protein involved in host cell invasion and disarming the cell's defense. Delivery of YopB to the host cell is regulated by the Type III secretion system (T3SS) (i.e. injectisome). The needle tip of the injectisome contains the LcrV protein. When *Y. pestis* comes in contact with a cell membrane, the injectisome forms a pore through the membrane to facilitate the diffusion of effector proteins into the host cell. Multiple lines of evidence suggest that pores are formed only through the direct interaction of YopB with LcrV[15, 16].

The FCS diffusion times of free LcrV (τ_f ; Figure 2A, black curve) and fully bound LcrV (τ_b; [YopB] = 10 μM) were found to be ≈ 140 μs and ≈ 630 μs, respectively. As no measurable change in diffusion time was detected above [YopB] = 1 μM (Figure 2, green curve), LcrV was assumed to be completely bound at

[YopB] = 10 μM. The diffusion times of free and bound LcrV were determined by fitting the autocorrelation curve to a one component model ($\chi^2 \approx 1$ for each diffusion time; Online Methods). These diffusion times correspond to average hydrodynamic radii of 2.5 nm for free LcrV and 11.1 nm for the Lcrv + YopB-NLP complex, as calculated by the Einstein-Stokes equation. No change in diffusion time was found when LcrV was incubated with NLP lacking the YopB protein (data not shown), suggesting that LcrV alone is unable to interact with a lipid bilayer. To extract the dissociation constant (K_D), a titration was performed over a range of YopB concentrations (10 pM - 1 μM). Having determined the values of the diffusion times for free (τ_f) and bound (τ_b) protein, we fitted the autocorrelation curves to a two species correlation function (Online Methods). The only varying parameters were the correlation amplitudes α (free protein) and β (bound protein), providing the fraction bound at a specific concentration, $F = \frac{\beta}{\alpha+\beta}$. Intermediate binding was observed between 10 nM and 100 nM, as two correlation components are resolved. At [YopB]=50 nM, the ratio β/α was 1.5,indicating that over half of LcrV was bound. For the two component model in these intermediate cases, the χ^2 value was between 1 and 1.3, indicating a good fit. In contrast, fitting the data to a one component model resulted in a poor fit ($\chi^2 > 7$), justifying the use of the two species model.

We used the receptor-ligand model given by $R + L \underset{k_{off}}{\overset{k_{on}}{\rightleftarrows}} RL$. Binding curves were fitted to a Hill equation $y = \frac{x}{K_D+x}$ where y is the fraction of bound LcrV, x is the YopB concentration, and $K_d = \frac{k_{off}}{k_{on}}$ the dissociation constant. Fitting this model with a least squares algorithm, we extracted $K_d \approx 20.5 \pm 2.0$ nM. To quantify the statistical error, three measurements were recorded for two minutes, and the whole titration was repeated twice. Importantly, these data provide not only a quantitative binding affinity for the YopB-LcrV interaction, but support the hypothesis that LcrV requires direct interaction with YopB, not just a lipid bilayer, to promote pore formation.

We demonstrate that FCS can readily perform quantitative binding measurements of interactions between labeled soluble proteins and unlabeled membrane proteins inserted into NLPs. FCS provides the ability to simultaneously detect the presence of both free and bound species in a solution-based, native-like environment without the need for surface immobilization of the cognate proteins. Furthermore, this approach directly measures the effects of binding on the movement of bound proteins with single-molecule sensitivity, allowing the extension of this methodology to include more information, such as stoichiometry (i.e. antibunching[17]), distance information (i.e. FRET)[18], and two-color fluorescence cross-correlation spectroscopy (FCCS)[19, 20]. Cell-free co-expression of both membrane protein and apolipoprotein components represents a facile methodology for producing soluble, NLP-supported membrane proteins at high yield. In addition, expressing the soluble cognate proteins with an EGFP label provides a simple path to obtaining fluorescent, single-labeled soluble proteins compatible with FCS. The combination of FCS with NLP technology provides not only key data for modeling the invasion process of a bacterial pathogen, but also serves as a model for studying interactions between other soluble and membrane proteins. Such methods have been lacking, yet are critical for understanding interaction networks, *e.g.* signal transduction cascades. In conclusion, the coupling of

these two methodologies provides a facile yet powerful tool to complement traditional approaches to probe interactions with membrane proteins, and addresses key bottlenecks of accessibility to membrane proteins as well as quantitative, single-molecule measurements.

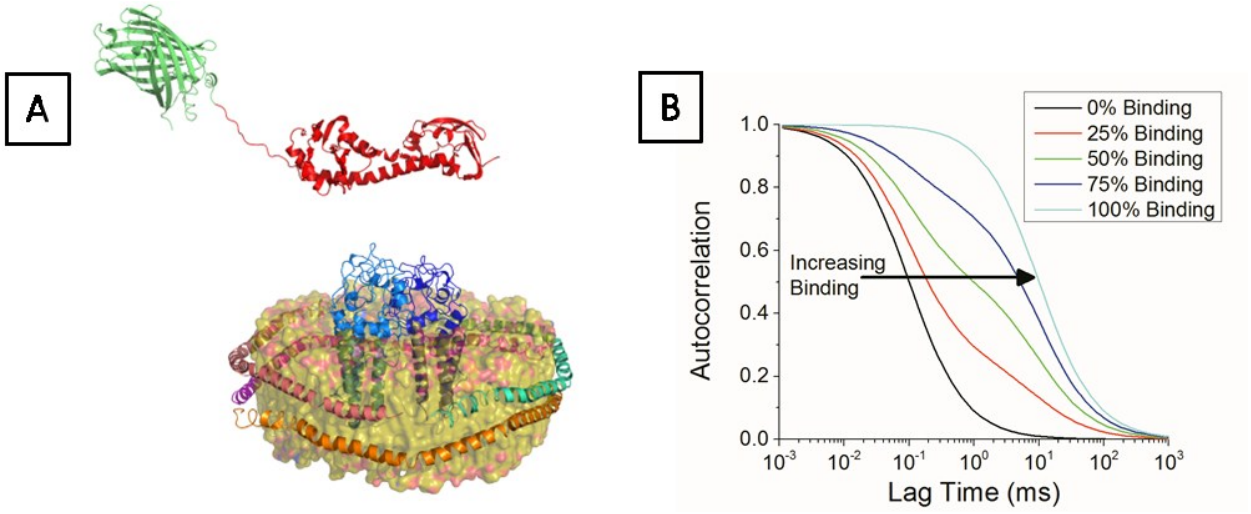

Figure 1. A) Model of YopB (blue) inserted into a 10 nm NLP complex and LcrV (red) labeled with EGFP (green). The molecular weight used in this model is: LcrV (35kDa), EGFP (27kDa), YopB (42kDa, monomer), and NLP-YopB complex (~250kDa). The small LcrV binds to the much larger YopB-NLP complex which shifts the autocorrelation curves to longer diffusion times. B) Theoretical autocorrelation curves expected for a series of titration experiments measured using FCS. Increased binding is measured as an increase in diffusion time. For instances of intermediate binding, two diffusion components are detectable (red, green and blue curves).

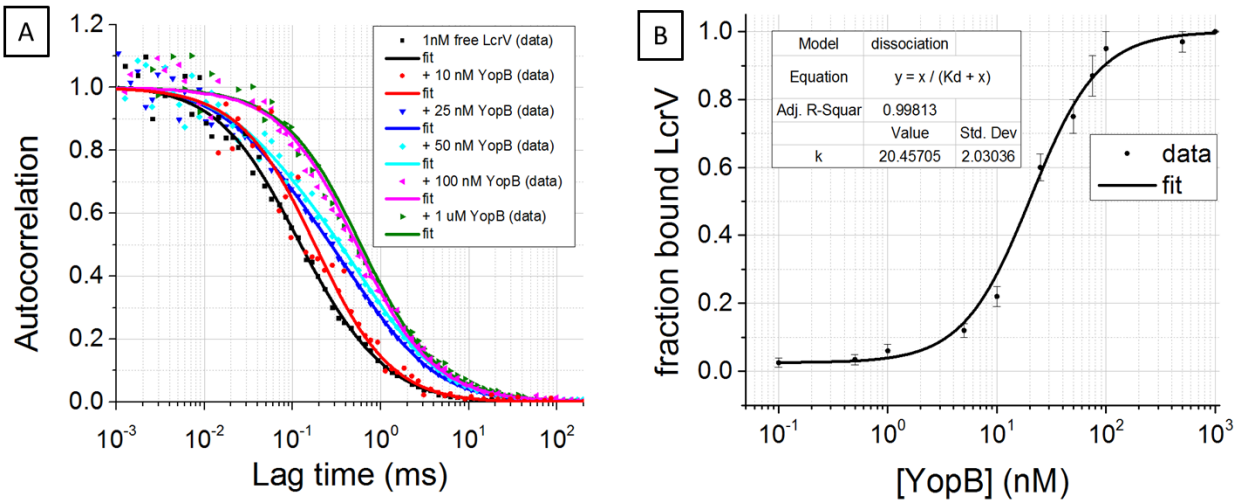

Figure 2. A) FCS autocorrelation curves of 1 nM EGFP-labeled LcrV protein in the absence and presence of YopB at increasing concentrations. The diffusion time of freely diffusing LcrV is $\boldsymbol{\tau_{D,free} = 140\ \mu s}$. The shape of the autocorrelation curves change above [YopB] = 25 nM due to intermediate binding where a significant portion is dominated by a second diffusing component.

At [YopB] = 1 μM where LcrV is completely bound, the FCS curve is dominated by a single component. B) The fraction of bound LcrV as a function of YopB concentration (log scale). This fraction is calculated by fitting the FCS curves shown in Fig. 2A with Equation 2 (Online Methods). The dissociation constant extracted is $K_d \approx 20.45 \pm 2.0$ nM. Error bars represent average over six FCS measurements.

Acknowledgements

Work was performed under the auspices of the U.S. Department of Energy under contract number DE-AC52-07NA27344 to Lawrence Livermore National Laboratory and supported by funding from the Laboratory Directed Research and Development program.

References

1. Yildirim, M.A., Goh, K.I., Cusick, M.E., Barabási, A.L. & Vidal, M. Drug-target network. *Nature biotechnology* **25**, 1119 (2007).
2. Lalonde, S. et al. Molecular and cellular approaches for the detection of protein–protein interactions: latest techniques and current limitations. *The Plant Journal* **53**, 610-635 (2008).
3. Nath, A., Atkins, W.M. & Sligar, S.G. Applications of phospholipid bilayer nanodiscs in the study of membranes and membrane proteins. *Biochemistry* **46**, 2059-2069 (2007).
4. Segrest, J.P. et al. A detailed molecular belt model for apolipoprotein A-I in discoidal high density lipoprotein. *J Biol Chem* **274**, 31755-31758 (1999).
5. Leitz, A.J., Bayburt, T.H., Barnakov, A.N., Springer, B.A. & Sligar, S.G. Functional reconstitution of beta2-adrenergic receptors utilizing self-assembling Nanodisc technology. *Biotechniques* **40**, 601 (2006).
6. Gao, T. et al. Characterization of de novo synthesized GPCRs supported in nanolipoprotein discs. *PloS one* **7**, e44911 (2012).
7. Nath, A., Grinkova, Y.V., Sligar, S.G. & Atkins, W.M. Ligand binding to cytochrome P450 3A4 in phospholipid bilayer nanodiscs: the effect of model membranes. *J Biol Chem* **282**, 28309-28320 (2007).
8. Alami, M., Dalal, K., Lelj-Garolla, B., Sligar, S.G. & Duong, F. Nanodiscs unravel the interaction between the SecYEG channel and its cytosolic partner SecA. *The EMBO journal* **26**, 1995-2004 (2007).
9. Ryan, R.O. Nanodisks: hydrophobic drug delivery vehicles. *Expert Opin Drug Deliv* **5**, 343-351 (2008).
10. Cappuccio, J.A. et al. Cell-free co-expression of functional membrane proteins and apolipoprotein, forming soluble nanolipoprotein particles. *Molecular & Cellular Proteomics* **7**, 2246-2253 (2008).

11. Gao, T. et al. Characterizing diffusion dynamics of a membrane protein associated with nanolipoproteins using fluorescence correlation spectroscopy. *Protein Science* **20**, 437-447 (2011).
12. Nath, A. et al. Single-molecule fluorescence spectroscopy using phospholipid bilayer nanodiscs. *Methods in enzymology* **472**, 89-117 (2010).
13. Elson, E.L. Fluorescence correlation spectroscopy: past, present, future. *Biophysical journal* **101**, 2855-2870 (2011).
14. Meseth, U., Wohland, T., Rigler, R. & Vogel, H. Resolution of fluorescence correlation measurements. *Biophys J* **76**, 1619-1631 (1999).
15. Andrews, G. et al. Protective Efficacy of RecombinantYersinia Outer Proteins against Bubonic Plague Caused by Encapsulated and Nonencapsulated Yersinia pestis. *Infection and immunity* **67**, 1533-1537 (1999).
16. Edqvist, P.J., Aili, M., Liu, J. & Francis, M.S. Minimal YopB and YopD translocator secretion by Yersinia is sufficient for Yop-effector delivery into target cells. *Microbes and infection* **9**, 224-233 (2007).
17. Ly, S. et al. Stoichiometry of Reconstituted High-Density Lipoproteins in the Hydrated State Determined by Photon Antibunching. *Biophysical journal* **101**, 970-975 (2011).
18. Laurence, T.A. et al. Motion of a DNA sliding clamp observed by single molecule fluorescence spectroscopy. *Journal of Biological Chemistry* **283**, 22895 (2008).
19. Schwille, P., Meyer-Almes, F.J. & Rigler, R. Dual-color fluorescence cross-correlation spectroscopy for multicomponent diffusional analysis in solution. *Biophysical journal* **72**, 1878-1886 (1997).
20. Ly, S. et al. Binding of Apolipoprotein E Inhibits the Oligomer Growth of Amyloid-β Peptide in Solution as Determined by Fluorescence Cross-correlation Spectroscopy. *Journal of Biological Chemistry* **288**, 11628-11635 (2013).
21. Sawasaki, T. et al. A bilayer cell-free protein synthesis system for high-throughput screening of gene products. *FEBS letters* **514**, 102-105 (2002).
22. Segelke, B.W. et al. Laboratory scale structural genomics. *Journal of structural and functional genomics* **5**, 147-157 (2004).
23. Lobley, A., Sadowski, M.I. & Jones, D.T. pGenTHREADER and pDomTHREADER: new methods for improved protein fold recognition and superfamily discrimination. *Bioinformatics* **25**, 1761-1767 (2009).
24. Eicken, C. et al. Crystal structure of Lyme disease variable surface antigen VlsE of Borrelia burgdorferi. *Journal of Biological Chemistry* **277**, 21691-21696 (2002).
25. Mei, X. & Atkinson, D. Crystal structure of C-terminal truncated apolipoprotein AI reveals the assembly of high density lipoprotein (HDL) by dimerization. *Journal of Biological Chemistry* **286**, 38570-38582 (2011).
26. Derewenda, U. et al. The Structure of Yersinia pestis V-Antigen, an Essential Virulence Factor and Mediator of Immunity against Plague. *Structure* **12**, 301-306 (2004).
27. Yang, F., Moss, L.G. & Phillips Jr, G.N. The molecular structure of green fluorescent protein. *Dept. of biochemistry and cell biology, Rice University* (1997).

Online Methods

Plasmids

The truncated form of Apo A1 (Δ1-49) or ΔA1 was cloned as previously described in pIVEX2.4d using NdeI and SmaI restriction sites[10]. This vector also contains a His-tag for nickel affinity purification. The YopB sequence from *Yesinia pestis* CO92 were cloned as described previously[16, 21, 22]. Briefly the gene of interest was PCR amplified with primers containing restriction sites for *Nde*I and *BamH*I and cloned into a modified pETBlue (Novagen) C-terminal His6 tagged system. YopB was subsequently sub-cloned directionally into the His-tagged pIVEX 2.4b vector (Roche). LcrV-GFP was PCR-amplified with primers containing *Nde*I and *BamH*I resctriction sites and cloned into a GFP-folder expression plasmid as described previously(5).

Cell-free Reactions

Preparative scale reactions (1 mL) were carried out using 5Prime's RTS 500 ProteoMaster Kit. For co-expression of YopB-NLPs the plasmid DNA was added in the following amounts 10 μg of YopB and 2 μg of ΔA1. "Empty"-NLPs (no co-expressed Yop protein) were prepared using 10 μg of ΔA1 DNA. To the lysate/DNA mixture DMPC vesicles (2 mg/mL) were added, see below. LcrV-GFP reactions were prepared with 15 μg LcrV-GFP plasmid. The reactions were incubated at 30 °C for 18 hrs. at 300 rpm, in a New Brunswick Shaker Incubator.

Lipid preparation

Small unilamellar vesicles of DMPC (liposomes) were prepared by probe sonicating a 68 mg/mL aqueous solution of DMPC until optical clarity is achieved; typically 15 min is sufficient. A 2 min. centrifugation step at 13700 RCF removed any metal contamination from the probe tip. The individual lipid component was added to the cell-free reaction at a concentration of 2 mg/mL.

Affinity purification of NLP complexes

Immobilized metal affinity chromatography was used to isolate the protein complexes of interests from the cell-free reaction mixture based on the affinity of the N-terminal poly-His tag. The cell-free fraction was mixed at 4 °C for 1 hr. with 1 mL of SuperFlow Ni-NTA resin (Qiagen) pre-equilibrated with PBS (50 mM Na_2HPO_4, 300 mM NaCl, pH 8.0) under native conditions in a 5 mL capped column. The column was washed with 6 column volumes of 20 mM imidazole in PBS buffer. The His-tagged proteins of interest were eluted in six 1mL fractions with 400 mM imidazole in PBS buffer. All elutions were combined, concentrated and buffer exchanged into PBS using a 7K MWCO molecular weight Slide-A-Lyzer dialysis cassette (ThermoFisher). Protein concentrations were determined using Quant-iT Protein Assay (LifeTechnologies).

FCS Measurements

Experiments were conducted with a 470nm pulsed laser (80ps pulse width, 20Mhz, Picoquant) focused to a diffraction limited spot with 100x N.A.=1.4 oil objective. The average power is 50 μW at the sample. The fluorescence emission is spectrally filtered with bandpass filters (HQ520/40m, Chroma Technology), and detected by two avalanche photodiode detectors (PDM Series, Micro Photon Devices). The signals were processed by time-correlated single-photon counting (PicoHarp300, PicoQuant), operating in time-tagged time-resolved (TTTR) mode. The TTTR mode of the data acquisition records the photon arrival time from the last excitation pulse (micro-time) with 50 ps relative time resolution, and the photon arrival time from the start of the experiment (macro-time) with 100 ns absolute time resolution. TCSPC of separate detection channels allows for the temporal analysis of all detected photons. Autocorrelations were calculated and fitted using SymPhoTime software (PicoQuant).

FCS Analysis

In FCS statistical fluctuations of the fluorescence intensity $\delta I(t)$ around a mean intensity $\langle I \rangle$ are recorded. These fluctuations result from changes in the number of fluorescent molecules diffusing through a femtoliter sized laser volume. Performing an autocorrelation analysis of these fluctuations, which measures the self-similarity as a function of delay, provides information regarding the molecule's concentration and its diffusion coefficient. The autocorrelation function for a 2D translational diffusion through a confocal volume is:

$$G(\tau) = \frac{1}{N} \frac{1}{1 + \frac{\tau}{\tau_D}} \tag{1}$$

with *N* the number of fluorescent molecules, $\tau_D = \frac{\omega^2}{4D}$ the diffusion time, and D the diffusion coefficient, and ω is the lateral beam waist.

For binding interactions, the amount of ligand in the free and bound state can be separated by their diffusion time and quantified as a function of concentration. The fraction of bound protein is calculated by fitting the correlation to two components. The first component $f(\tau)$ is the correlation of LcrV alone. The second component $g(\tau)$ is the correlation when LcrV is bound to YopB-NLP.

The total correlation function is:

$$h(\tau) = \alpha f_o(\tau) + \beta g_o(\tau) \tag{2}$$

where

$$f_o(\tau) = \frac{1}{1 + \frac{\tau}{\tau_f}} \quad \text{and} \quad g(\tau) = \frac{1}{1 + \frac{\tau}{\tau_b}} \tag{3}$$

and α and β are amplitudes of the correlation function for free and bound protein. The ratio $F = \frac{\beta}{\alpha+\beta}$ gives the fraction bound.

Modeling of LcrV – YopB

The amino acid sequence of YopB was submitted to pGenTHREADER[23] and identified to have a similar fold to the lipoprotein VlsE, variable surface antigen of *Borrelia burgdorferi*. Residues 125 – 374 of YopB were modeled after the dimer crystal structure of VlsE (PDB: 1L8W)[24]. The YopB dimer was inserted into a lipid bilayer disc 10 nm in diameter and lipids within 4 angstroms of a protein atom were deleted. The belt proteins for the NLP were constructed from human apolipidprotein A-1 (PDB: 3R2P)[25]. The V-antigen (LcrV protein) from Yersinia pestis with the GFP construct was modeled using the crystal structures of 1R6F[26] and 1GFL[27], respectively.

References